

Quantum Monte Carlo calculations of phonon-assisted luminescence from polyexcitons in Si

A. C. Cancio and Yia-Chung Chang

Department of Physics and Materials Research Laboratory, University of Illinois at Urbana-Champaign, Urbana, Illinois 61801

(Received 6 April 1994)

We calculate the line shapes and total oscillator strengths for phonon-assisted recombination from polyexcitons, complexes involving two, three, or four excitons, in Si. Line shapes are determined from ground-state to ground-state transition matrix elements, using variationally determined correlated wave functions. Transition matrix elements are calculated with Monte Carlo methods. We find that about 90% of the total oscillator strength in the decay of the larger complexes can be accounted for by the ground-state to ground-state mechanism, obviating the need for consideration of excited final states. The line shapes and widths of the larger complexes are similar to that of the biexciton, with oscillator strength per exciton increasing slightly with increasing complex size due to many-body effects.

I. INTRODUCTION

Recombination luminescence has been an important source of information about excitonic states in indirect-gap semiconductors. The principal source of luminescence from indirect-gap semiconductors is phonon-assisted luminescence, or PAL, in which the momentum required to recombine an electron and hole across an indirect gap is taken up by the absorption or emission of a phonon. The PAL line shape is closely related to the momentum distribution of electron-hole pairs in the crystal and thus serves as a useful probe of the structure of electron-hole excited states in these semiconductors. PAL has proven to be one of the most important tools in the study of excitonic states in Si and Ge. In particular, it has been used to prove the existence of biexcitons in Si (Ref. 1) and in uniaxially stressed Si (Ref. 2) and Ge,³ and has provided the first clear evidence of the electron-hole liquid (EHL)^{4,5}. PAL line shapes and oscillator strengths can be used to obtain estimates of the binding energy and radii and concentrations of small exciton complexes such as the biexciton,⁶ and the band-gap renormalization, density, and electron-hole enhancement factor of the EHL.^{7,8} PAL luminescence has also been a crucial tool in determining the phase diagram of macroscopic excitonic states in these materials under equilibrium conditions.

A wide variety of excitonic states are observable in Si, providing a rich field for the study of many-body and few-body Coulombic systems.⁹ At low temperatures, a simple liquid-gas phase diagram has explained the observed thermodynamics of electrons and holes successfully. The phase transition is of interest because it is not only a liquid-gas transition but a metal-insulator one as well, from a highly metallic quantum liquid of ionized electrons and holes to a weakly ionized gas phase consisting mostly of excitons coexisting with small populations of free carriers and small complexes or molecules consisting of more than one electron-hole pair. The low-temperature phases have been studied extensively and

are theoretically well understood.¹⁰ The liquid phase is highly metallic, with average nearest neighbor distances (estimated as the radius of the sphere containing the average volume per particle) of about 0.5 exciton Bohr radii at zero pressure ($r_s = 0.5$), and is well suited to high density perturbation methods. The saturation density of the gas phase is low enough to consider the exciton gas as ideal.

At temperatures near the critical temperature of the EHL (~ 20 K in Si), the electron-hole phase diagram at intermediate densities is as yet poorly understood. At densities corresponding to $r_s > 1.0$ the electron-hole system occupies a transitional regime between the potential-energy-dominated exciton gas and the highly degenerate, kinetic-energy-dominated regime of the electron-hole liquid or plasma, in which many-body correlations are important and standard mean-field approaches fail. Since the EHL remains at metallic densities up to the critical point of the liquid-gas transition, it has been conjectured that at temperatures near the critical temperature a metal-insulator transition should occur at a density lower than the saturated gas density of the liquid-gas transition.¹¹ As there are indications that this transition could be a first-order one, there might then be two distinct first-order phase transitions and critical points for the system. This situation has not been seen in liquid metals, such as liquid Hg;¹² on the other hand, the EHL is unique among metallic liquids in having a liquid-gas critical point that is well within the metallic regime with $r_s < 1.00$.^{11,13}

Recently, time-resolved photoluminescence studies of highly photoexcited Si (Ref. 14) and Ge (Ref. 15) at temperatures near the critical point of the EHL have reported the anomalous time dependence of the PAL line shape of an expanding electron-hole plasma. This has been interpreted as evidence of the existence of a second metallic condensed phase of electron-hole pairs existing above the critical temperature of the EHL and at lower densities than the EHL critical density in these systems.

The luminescence feature has also been interpreted as

coming from polyexcitons,¹⁶ or complexes of more than two excitons bound to each other. Such large exciton complexes should be stably bound in Si and Ge due to the highly degenerate conduction and valence band edges in these materials, reducing the antibinding effects of Fermi statistics. However, the thermodynamics of the exciton gas inhibits the formation of these larger complexes except at fairly high densities. Luminescence from polyexcitons formed out of the expanding plasma in this experiment would inhabit roughly the same region of the photoluminescence spectrum and exhibit similar time dependence as that of the condensed plasma line reported. A recent study of green-light photoluminescence associated with simultaneous recombination of two electron-hole pairs has confirmed the existence of polyexcitons (PE's) in Si,¹⁶ with binding energies consistent with the PE interpretation of the anomalous phonon-assisted luminescence. However, it is difficult to determine unambiguously the relative importance of electron-hole plasma versus large molecular complexes in determining the PAL spectrum in this region.

Theoretically the phonon-assisted luminescence of polyexcitons is interesting for several reasons. The PAL provides an experimental measurement of the momentum distribution of excitons and interparticle correlations in excitonic systems. In particular the line shape of the X_2 observed at low temperature (~ 2 K) provides clean data that can be directly tied to exciton-exciton correlations in the complex.¹ Thus one has, at least for the biexciton, a fairly detailed source of experimental information on the biexciton ground state against which one may test various theories. Data from larger PE's have not been observed at temperatures low enough for clean observation; the high-temperature data (above T_c for the EHL, ~ 20 K in Si) are hard to resolve because of the kinetic energy broadening of photoluminescence lines. Nevertheless, theoretical predictions of the line shape and oscillator strength of PAL luminescence from polyexcitons would be useful in assessing the validity of the PE interpretation of above- T_c luminescence at intermediate densities.

A line-shape calculation for the biexciton or X_2 was attempted by Cho,⁶ who showed that the form of the line shape could be determined from the effective mass envelope of the X_2 ; he used a simple model for exciton-exciton correlations to derive a form for the empirical fit of the line shape. A more quantitative calculation of the effective-mass envelope matrix element for the X_2 line shape has been developed by Kulakovskii *et al.*² and Timofeev,¹⁷ using a generalization of the exciton absorption theory of Elliott¹⁸ and the variational theory of Brinkman, Rice, and Bell.¹⁹ No calculations have been performed for the X_3 and X_4 complexes to our knowledge.

In general the quantitative calculation of the line shape for the polyexciton is quite difficult, since it can depend quite sensitively on the wave function. Accurate variational wave functions for the X_2 have been difficult to find given the very small binding energy which one is attempting to account for and the important role of interparticle correlations in accounting for this binding en-

ergy. The variational calculation of Ref. 18 obtained only 50% of the binding energy for the X_2 as compared with an exact Green's function Monte Carlo (GFMC) projection method.²⁰ Recently we have used a modified Jastrow wave function to calculate the ground-state wave function of PE's employing the variational Monte Carlo (VMC) method to calculate integrals,²¹ obtaining about 85% of the GFMC ground-state energy for the X_2 .

In this paper we report the theoretical calculation of oscillator strengths and line shapes of the PAL spectra of polyexcitons. We use the variational wave function developed in a previous paper²¹ and a generalization of the overlap matrix element used in Ref. 2. Matrix elements are calculated using Monte Carlo importance sampling methods. The rest of the paper is organized as follows. The second section gives a description of the general theory of PE's and their recombination through phonon-assisted luminescence, and Sec. III outlines the Monte Carlo method used. Section IV outlines our results and a brief discussion of errors, with a final conclusion in Sec. V.

II. THEORY OF PHONON-ASSISTED LUMINESCENCE FROM POLYEXCITONS

A. Polyexciton Hamiltonian

In the limit of weak interactions, one can represent the single particle band excitations of a semiconductor through the effective-mass approximation, in which they are treated as point particles in an effective medium. The Hamiltonian describing a complex of N electrons (with coordinate subscripts i and i' and coordinates \mathbf{r}) and holes (subscripts j and j' , coordinate \mathbf{s}) in this effective medium is given as

$$H = \sum_{i=1}^N \left(-\frac{\nabla_i^2}{2m_e} \right) + \sum_{j=1}^N \left(-\frac{\nabla_j^2}{2m_h} \right) + \sum_{i=1}^N \sum_{i' < i}^N \frac{e^2}{\epsilon_0 r_{ii'}} + \sum_{j=1}^N \sum_{j' < j}^N \frac{e^2}{\epsilon_0 s_{jj'}} - \sum_{i=1}^N \sum_{j=1}^N \frac{e^2}{\epsilon_0 |\mathbf{r}_i - \mathbf{s}_j|}. \quad (1)$$

The effective masses m_e and m_h are determined by taking the spherically averaged curvature of the conduction band at its minimum and the valence band maximum, respectively. The interaction between particles is taken to be the Coulomb interaction, screened by the static dielectric constant ϵ_0 , suitable for weakly bound complexes. This equation is formally equivalent to that of a finite complex of electrons and positrons interacting through the Coulomb equation. With a suitable choice of units, the exciton Rydberg $E_X = \mu_{eh} e^4 / 2\epsilon^2 \hbar^2$, and exciton Bohr radius $a_X = \hbar^2 / (2\mu_{eh} e^2 / \epsilon)$, one obtains a dimensionless form of Eq. (1),

$$H = \sum_{i=1}^N \left(-\frac{1}{1+\sigma} \nabla_i^2 \right) + \sum_{j=1}^N \left(-\frac{\sigma}{1+\sigma} \nabla_j^2 \right) + \sum_{i=1}^N \sum_{i' < i}^N \frac{2}{r_{ii'}} + \sum_{j=1}^N \sum_{j' < j}^N \frac{2}{s_{jj'}} - \sum_{i=1}^N \sum_{j=1}^N \frac{2}{|\mathbf{r}_i - \mathbf{s}_j|}. \quad (2)$$

In this case the only crystal-dependent parameter involved is the electron-hole mass ratio $\sigma = \frac{m_e}{m_h}$, equal to 1 for the electron-positron system. The exciton Rydberg obtained in the spherical approximation, 12.88 meV, is in fairly good agreement with the observed exciton ground-state energy of 14.7 meV.

Despite the formal equivalence between the spherical effective-mass Hamiltonian for electrons and holes in Si and that for electrons and positrons, there is an important difference between the two situations, the degenerate nature of the band edges of both the conduction and valence bands, which leads to quite different physical behavior. For Si the uppermost valence band has a fourfold degenerate $J = 3/2$ -like band maximum formed from spin-orbit coupled p orbitals and a conduction band with six equivalent energy minima at nonzero wave vectors in the [100] and equivalent directions. As a result, up to four holes (or the filling of the $j = 3/2$ valence band edge) and up to 12 electrons (up to the filling of the six conduction band valleys) may inhabit the lowest lying single particle states of a particular complex before Fermi statistics force the occupation of states with higher kinetic energy. The band-edge degeneracy results in the stability of complexes of three, four, and possibly more electron-hole pairs, complexes whose analogs in positron-electron systems would not be bound. Complexes of up to five pairs have been observed in Si with measured exciton binding energies of 1.36, 3.83, and 6.34 meV for the two-, three-, and four-pair complexes, respectively.¹⁶

B. Wave function

Since the binding energies of the polyexciton complexes are small compared to that of the exciton Rydberg, a reasonable starting point for building a variational wave function is that of a system of N free excitons:

$$\psi_{NX}(R) = \sum_P \prod_{i=1}^N \phi_X^0(|\mathbf{r}_i^e - \mathbf{s}_{P(i)}^h|), \quad (3)$$

where ϕ_X^0 is the exciton ground state and the sum \sum_P is over the permutation of electrons and holes. For complexes of less than four holes (and 12 electrons), the spatial component of the ground state is symmetric.

In order to include the correlations induced by the Coulomb interactions between excitons, additional pair correlation functions are introduced: f_{ee} , f_{eh} , and f_{hh} , for electron-electron, electron-hole, and hole-hole interactions respectively. In addition the excitonic wave function ϕ_X^0 is replaced by a form f_X which allows for the possibility of screening of the exciton by the other particles. The resulting correlated wave function may be written as

$$\psi_{X-J}(R) = \psi_J(R) \sum_P \prod_{i=1}^N \eta(|\mathbf{r}_i^e - \mathbf{s}_{P(i)}^h|), \quad (4)$$

where

$$\eta(r) = f_X(r)/f_{eh}(r) \quad (5)$$

and

$$\begin{aligned} \psi_J(R) = & \prod_{i=1}^{N_e} \prod_{i' < i}^{N_e} f_{ee}(r_{ii'}) \\ & \times \prod_{j=1}^{N_h} \prod_{j' < j}^{N_h} f_{hh}(s_{jj'}) \prod_{i=1}^{N_e} \prod_{j=1}^{N_h} f_{eh}(|\mathbf{r}_i - \mathbf{s}_j|). \end{aligned} \quad (6)$$

Here $R = (\mathbf{r}_1^e, \dots, \mathbf{r}_{N_e}^e; \mathbf{s}_1^h, \dots, \mathbf{s}_{N_h}^h)$, and r_{ij} is the distance between the i th and j th particles. The forms for the pair correlation functions f_{ee} , f_{hh} , f_{eh} , and f_X are described in Ref. 21.

Variational calculations for the ground state of the electron-hole liquid have been made in a fermion hypernetted chain approach using the Jastrow wave function multiplied by electron and hole Slater determinants.²² In the macroscopic homogeneous liquid, this approximation is flexible enough to obtain exact limiting behavior on the long-wavelength and short-wavelength behavior of the partial structure functions. Ground-state energies of the Fermi hypernetted chain approach were quite close to those using VMC and GFMC methods for the electron gas.

For a finite electron-hole system, the Jastrow wave function lacks the flexibility to allow for the unscreened excitonic correlation one expects for electron-hole pairs at the surface of the polyexciton in addition to the screened electron-hole correlation appropriate for high density regions. The use of the free exciton wave function ψ_{NX} allows the incorporation of this kind of correlation from the start. In particular, one obtains the correct limiting behavior of the wave function in the limit that any given electron-hole pair is taken away from the complex. The use of this form improves the variational estimate of the binding energy considerably as compared to that from the Jastrow wave function. We obtain 2.053(3) Ry for the biexciton total energy as compared to the exact GFMC result of 2.060(1) Ry,²⁰ and 2.019(5) Ry using the Jastrow form alone.

C. Theory of phonon-assisted luminescence

In indirect-gap semiconductors the first-order optical emission process with the $\Delta \mathbf{k} = \mathbf{0}$ selection rule has a very low probability for most excited states of the semiconductor, typically involving a few electrons and holes concentrated near the band edges. Conservation of momentum requires either the electron or the hole or both to have a k vector far from its band edge, involving electronic states with a very low probability of occupation. Recombination is possible through various second-order processes, usually involving the simultaneous emission or absorption of a phonon to conserve momentum. The phonon momentum contributes an additional degree of freedom which relaxes the $\mathbf{k} = \mathbf{0}$ selection rule and allows a continuum of transitions from any given initial state or to any final state, contributing to an enhancement of the oscillator strength that partly compensates for the reduced second-order matrix element. The phonon has the desirable property of acting as a probe of the momentum

distribution of the electronic state in question, with the results of the “experiment” observed by the emission of light.

In comparison to the recombination line of the free exciton (FE), the PE line experiences broadening as a result of the more complicated internal structure of the complex. That is, in addition to the high-energy Boltzmann tail characteristic of the FE line, the PE line has an additional low-energy tail from processes in which the remaining $N - 1$ particles absorb some of the energy of the initial complex. As observed by Cho,⁶ this recoil effect is characterized largely by the long-wavelength correlations between the recombining pair and the rest of the system, which are described by the effective-mass envelope.

In detail, the phonon-assisted process $X_N \rightarrow X_{N+1} + h\nu + \hbar\Omega$ is described as follows. As phonon emission and absorption have threshold energies separated by $2\hbar\Omega(K_0)$ we need consider only emission here. We consider an initial state of a polyexciton with N electron-hole pairs inhabiting various conduction band minima at \mathbf{K}_0^i and the degenerate valence band at $K = 0$. The total momentum of the system is $\sum_i^N \mathbf{K}_0^i + \mathbf{K}$, i.e., the sum over the momenta of the conduction band minima plus a small deviation in momentum due to the center-of-mass motion. The total energy of the complex is $NE_{\text{gap}} + \hbar^2 K^2 / 2M_X N + E_0[X_N]$, that is, the minimal energy required to create N electron-hole pairs across an energy gap E_{gap} , plus the kinetic energy of a complex with total mass NM_X , plus the internal energy $E_0[X_N]$ of the complex in its ground state. In a typical second-order perturbation theory approach, an electron assumed to be in valley 1 is scattered by the emission of a phonon of momentum $\mathbf{q} - \mathbf{K}_0^1$ to a point in k space near the valence band maximum. Subsequently, an electron-hole pair recombines emitting a photon with zero momentum and energy $h\nu$. The final state consists of $N - 1$ pairs with total momentum $\sum_i^N \mathbf{K}_0^i - \mathbf{K}_0^1 + \mathbf{k}$, and internally is assumed also to be in its ground state, with internal energy $E_0[X_{N+1}]$. Conservation of momentum and energy give the following relations:

$$\mathbf{q} = \mathbf{K} - \mathbf{k},$$

$$\begin{aligned} h\nu + \hbar\Omega(\mathbf{q} + \mathbf{K}_0^1) &= NE_{\text{gap}} + \frac{\hbar^2 K^2}{2M_X N} + E_0[X_N] \\ &\quad - (N - 1)E_{\text{gap}} - \frac{\hbar^2 k^2}{2M_X(N - 1)} \\ &\quad - E_0[X_{N-1}]. \end{aligned} \quad (7)$$

One can also consider a hole scattered by a phonon of nearly opposite momentum $\mathbf{q} + \mathbf{K}_0^1$ to recombine with an electron in valley 1. This process produces the same conservation relations and thus the same line shape and effective-mass overlap as the electron scattering process, but in general may have a different total oscillator strength.

The transition probability for phonon-assisted electron-hole recombination or creation for a given photon frequency

$$\begin{aligned} \gamma(\nu) &= 2\pi C(E_{\text{gap}}) \sum_K \sum_{\mathbf{k}} \sum_{\mathbf{q}} P(K) |M_{if}|^2 \\ &\quad \times \delta(E_i - E_f - \hbar\Omega_0 - h\nu). \end{aligned} \quad (8)$$

It involves the sum over final states (\mathbf{k}, \mathbf{q}) and an average over initial states K , occupied with probability $P(K)$. From this expression and the conservation laws (7) the line shape for phonon-assisted luminescence, after eliminating the phonon momentum \mathbf{q} by momentum conservation, can be written as

$$\begin{aligned} I(h\nu) &= \sum_K \exp\left(-\frac{\hbar^2 K^2}{2M_X N \kappa T}\right) \sum_{\mathbf{k}} |M(k, K, K_0)|^2 \\ &\quad \times \delta\left(\frac{\hbar^2 K^2}{2M_X N} - \frac{\hbar^2 k^2}{2M_X N - 1} + E[X_N] \right. \\ &\quad \left. - E[X_{N+1}] + E_{\text{gap}} - \hbar\Omega(K_0) - h\nu\right). \end{aligned} \quad (9)$$

The distribution of kinetic energies of the initial system $P(K)$ has been taken to be a standard Boltzmann distribution for an N -exciton complex with total mass NM_X derived from the total exciton mass $M_X = m_e + m_h$. We have ignored the possible thermal population of excited internal states in this expression. The PE systems here are characterized by large kinetic energies, and one expects excited states only on the order of the binding energy. At the temperatures relevant to the observation of PE's ($T > 10$ K) this effect could be important for the X_2 given its small binding energy, but in this case it may be more reasonable to consider these excited states as perturbations of the exciton line than as an intrinsic part of biexciton luminescence.

The characteristic width of the PE recombination line is expected to be on the order of the momentum distribution of electron-hole pairs in the polyexciton complex, which should be dominated by a small region $\delta q \sim 1/a_X$ about K_0 . Intrinsic phonon and optical matrix elements do not vary appreciably except over a momentum range on the order of the width of the Brillouin zone and thus may be considered as constants over the range of momenta important to the matrix element. The matrix element then can be separated into that for the phonon-assisted radiative recombination of an electron and hole situated at the conduction and valence band extrema, multiplied by an effective-mass overlap integral that incorporates the dependence of the matrix element upon the momentum of the pair:

$$|M(k, K, K_0)|^2 = |D_{cv}(K_0)|^2 |N(k, K)|^2. \quad (10)$$

An explicit derivation of this form using the effective-mass approximation is discussed in the Appendix. One obtains a generalization of Elliott's formula for radiative recombination of a direct-gap exciton,¹⁸ allowing for the simultaneous emission of a phonon to conserve momentum in the indirect-gap case.

The effective-mass overlap for phonon-assisted radiative recombination is given by

$$\begin{aligned}
N(\mathbf{k}, \mathbf{K}) &= N\left(\frac{N-1}{N}\mathbf{K} - \mathbf{k}\right) \\
&= \int d\mathbf{r}_1 d\mathbf{r}_2 \cdots d\mathbf{r}_N ds_1 ds_2 \cdots ds_N \phi_N(\mathbf{r}_1, \mathbf{r}_2, \dots, \mathbf{r}_N, \mathbf{s}_1, \mathbf{s}_2, \dots, \mathbf{s}_N) \\
&\quad \times e^{i\left(\frac{N-1}{N}\mathbf{K} - \mathbf{k}\right) \cdot (\mathbf{R}_1 - \mathbf{R}_{N-1})} \delta(\mathbf{r}_1 - \mathbf{s}_1) \phi_{N-1}(\mathbf{r}_2, \dots, \mathbf{r}_N, \mathbf{s}_2, \dots, \mathbf{s}_N),
\end{aligned} \tag{11}$$

where the \mathbf{r}_i and \mathbf{s}_i are electron and hole coordinates respectively, and ϕ_N and ϕ_{N-1} are the ground states of the N - and $N-1$ -exciton complexes. The center-of-mass coordinates for the recombining electron-hole pair, denoted \mathbf{R}_1 , and the $N-1$ remaining pairs, \mathbf{R}_{N-1} , are coupled through a recoil momentum $\frac{N-1}{N}\mathbf{K} - \mathbf{k}$. This recoil momentum describes, in the center-of-mass reference frame, the equal and opposite momenta of the two final-state components of the system. After integrating out the center of mass of the initial state, it is the only free variable remaining in the recombination process. The effective-mass matrix element essentially measures the probability that the X_N complex in its ground state can be found in a state with a coalesced electron-hole pair carrying momentum $\mathbf{q} = \mathbf{K} - \mathbf{k}$ and the other $N-1$ excitons forming an X_{N+1} ground state, in a sense providing a “snapshot” of the N -pair system at the instant of recombination.

Since we are calculating an overlap between the N -pair and $N-1$ -pair states, one may be led to think of the electron-hole pair recombination, with the ensuing creation of a Bose particle (the photon) in terms of the creation of some kind of quasiparticle (or quasipair) hole. In a Bose many-body system, the quasihole orbital formed by removing a particle from an N -particle complex can be

defined by taking the overlap between the ground states of the N - and $N-1$ -particle complexes:²⁴

$$\begin{aligned}
Q(\mathbf{r}) &= \frac{1}{\sqrt{Z}} \int d\mathbf{r}_2 \cdots d\mathbf{r}_N \phi_{N-1}(\mathbf{r}_2, \dots, \mathbf{r}_N) \\
&\quad \times \phi_N(\mathbf{r} - \mathbf{R}_{N-1}, \mathbf{r}_2, \dots, \mathbf{r}_N),
\end{aligned} \tag{12}$$

where a coefficient Z is included to normalize the orbital. In contrast to a fermion system, the ground state of a Bose system has only one quasiparticle state, reflecting, in a Hartree picture, the occupation of the same orbital by all the particles. Transitions involving the emission of particle in a weakly interacting system would then be dominated by the creation of this quasihole state, that is, be dominated by the ground-state to ground-state transition, with the total transition strength associated with the quasihole given by Z .²⁵

In our case, we are considering the decay of an electron-hole pair into a boson, within a system that is symmetric to the exchange of electron-hole pairs, so we should expect a similar behavior. If we consider the analogous expression for subtracting an electron-hole pair from an N -pair system we get

$$\begin{aligned}
Q_X(\mathbf{r}, \mathbf{s}) &= \frac{1}{Z_X} \int d\mathbf{r}_2 \cdots d\mathbf{r}_N ds_2 \cdots ds_N \phi_{N-1}(\mathbf{r}_2, \dots, \mathbf{r}_N, \mathbf{s}_2, \dots, \mathbf{s}_N) \\
&\quad \times \phi_N(\mathbf{r} - \mathbf{R}_{N-1}, \mathbf{r}_2, \dots, \mathbf{r}_N, \mathbf{s} - \mathbf{R}_{N-1}, \mathbf{s}_2, \dots, \mathbf{s}_N).
\end{aligned} \tag{13}$$

The recombination probability $|N(k)|^2$ can be rewritten in the formalism of a quasiparticle transition in terms of this “quasiexciton” orbital as

$$\begin{aligned}
|N(k)|^2 &= \frac{1}{\sqrt{Z_X}} \int d\mathbf{r} d\mathbf{r}' \exp[-i\mathbf{k} \cdot (\mathbf{r} - \mathbf{r}')] \\
&\quad \times Q_X^*(\mathbf{r}') Q_X(\mathbf{r}),
\end{aligned} \tag{14}$$

where the dependence of Q_X separately on the electron and the hole coordinate is suppressed, and the norm Z_X is given by an integral over $|Q(r)|^2$. The probability of the decay of the ground state of the N -exciton to an $N-1$ -exciton complex is thus determined by the probability of finding an electron-hole pair with momentum \mathbf{k} in the associated quasiexciton orbital, multiplied by an overall transition strength Z_X .

The possibility exists that the final state of the system is not an intact X_{N+1} complex in its ground state, but

that it absorbs internally some of the energy of the recombination process. Possible alternate final states are the $N-1$ complex in a bound excited state, states with one or more electron-hole pairs split off into free exciton states, and, at higher energies, states with free electrons and holes. Such states are in principle not as important to recombination as the ground state.

The effects of excited final states can be estimated from the integrated intensity of the phonon-assisted line:

$$I = \int I(h\nu) h d\nu. \tag{15}$$

For the range of frequencies important to the phonon-assisted process, the major contribution to this integral is from the effective-mass matrix element. The intensity I_{00} from ground-to-ground processes is given by an integral over final states \mathbf{k} of the ground-to-ground transition probability:

$$I_{00} = Z_X = \sum_{\mathbf{k}} |N^{00}(\mathbf{k})|^2. \quad (16)$$

In comparison, one can calculate the total intensity of the line by summing not only over the final-state center-of-mass momentum k , but over all possible internal states n as well. The total intensity I_{tot} is then simply given by

$$I_{\text{tot}} = \sum_n \sum_{\mathbf{k}} |N^{0n}(\mathbf{k})|^2, \quad (17)$$

where $N^{0n}(\mathbf{k})$ is the recombination matrix element between the N -exciton ground state and the n th excited state of the $(N-1)$ complex. The total intensity I_{tot} can be shown to be proportional to the electron-hole two-particle density at $r = 0$, $\rho_{eh}(0)$:

$$\begin{aligned} I_{\text{tot}} &= \sum_i^{N_e} \sum_j^{N_h} \langle \delta(\mathbf{r}_i - \mathbf{s}_j) \rangle \\ &= \rho_{eh}(0). \end{aligned} \quad (18)$$

The total radiative lifetime of the complex is then obtainable from I_{tot} .

The electron-hole two-particle density $\rho_{eh}(\mathbf{r})$ is defined as the average density of electron-hole pairs at a distance r from each other,

$$\rho_{eh}(|\mathbf{r} - \mathbf{s}|) = \int d^{\mathbf{r} + \mathbf{s}} \sum_i^{N_e} \sum_j^{N_h} \langle \delta(\mathbf{r}_i - \mathbf{r}) \delta(\mathbf{s}_j - \mathbf{s}) \rangle. \quad (19)$$

For a homogeneous system such as the EHL, the pair distribution function $g_{eh}(\mathbf{r})$ is obtained by dividing ρ_{eh} by the density of electrons squared. The lifetime is then usually written in terms of the density squared multiplied by the enhancement factor $g_{eh}(0)$.^{15,7} For the purposes of calculating $\rho_{eh}(0)$, it is convenient to define a two-particle density in the center-of-mass reference frame,

$$\tilde{\rho}_{eh}(\mathbf{r}, \mathbf{s}) = \sum_i^{N_e} \sum_j^{N_h} \langle \delta(\mathbf{r}_i - \mathbf{R}_N - \mathbf{r}) \delta(\mathbf{s}_j - \mathbf{R}_N - \mathbf{s}) \rangle. \quad (20)$$

The density of coalesced electron-hole pairs may be obtained as an integral over the electron and hole coordinates of this function for the case $\mathbf{r} = \mathbf{s}$:

$$\rho_{eh}(0) = \int d\mathbf{r} \tilde{\rho}_{eh}(\mathbf{r}, \mathbf{r}). \quad (21)$$

Representation of this quantity as an integral, rather than a limiting case of a function, allows for its calculation by Monte Carlo methods with greatly improved statistics.

III. MONTE CARLO CALCULATION OF MATRIX ELEMENTS

We have the calculation of the following overlap matrix element:

$$Q_X(\mathbf{r}, \mathbf{r}) = \frac{\int dR' dS' \psi_N^T(\mathbf{r}, R', \mathbf{r}, S') \psi_{N-1}^T(R', S')}{\|\psi_N^T\| \|\psi_{N-1}^T\|}. \quad (22)$$

As a shorthand the electron coordinates not involved in the transition are denoted collectively by R' , hole coordinates S' . This calculation is separated into that of the overlap integral using unnormalized trial wave functions obtained from a VMC calculation, and that of the normalization of each wave function. The unnormalized overlap calculation is sufficient to obtain the PAL line shape to within an arbitrary constant; the normalizations are necessary for a quantitative estimate of the total oscillator strength.

The overlap integral for the quasiexciton orbital for a given electron-hole pair in an N -pair complex, as a function of distance from the center of mass of the $(N-1)$ remaining pairs, can be done in the following manner.²⁴ One samples the final-state probability density $|\psi_{N-1}|^2$ over the $(N-1)$ -complex coordinates R' and S' by Monte Carlo techniques²⁶ and calculates the wave function for the N -pair complex formed by inserting an electron-hole pair at a distance r from the center of mass of the other particles. One obtains an estimate of the overlap up to a normalization factor by averaging the ratio of the N -pair to the $(N-1)$ -pair wave functions over a set of configurations $\{R', S'\}$,

$$O[\psi_N, \psi_{N-1}](r) = \left\langle \frac{\psi_N(\mathbf{r}, R', \mathbf{r}, S')}{\psi_{N-1}(R', S')} \right\rangle_{\{R', S'\}}. \quad (23)$$

Repeating the calculation for various values of r for the same set of configurations $\{R', S'\}$ yields an estimate of the quasiexciton orbital as a function of r .²⁷ At the same time, by taking the average expectation value of the ratio squared of the two wave functions, one obtains an unnormalized estimator $P[\psi_N, \psi_{N-1}]$ of the density of coalesced electron-hole pairs, $\tilde{\rho}_{eh}(\mathbf{r}, \mathbf{r})$, as a function of distance from the center of mass.

$$P[\psi_N, \psi_{N-1}](r) = \left\langle \left| \frac{\psi_N(\mathbf{r}, R', \mathbf{r}, S')}{\psi_{N-1}(R', S')} \right|^2 \right\rangle_{\{R', S'\}}. \quad (24)$$

A numerical integral over the coordinate r gives the total density of coalesced electron-hole pairs, $\rho_{eh}(0)$.

The normalized overlap and coalescent electron-hole density functions are

$$Q_X^N(\mathbf{r}, \mathbf{r}) = N^2 \frac{\|\psi_{N-1}\|}{\|\psi_N\|} O[\psi_N, \psi_{N-1}] \quad (25)$$

and

$$\tilde{\rho}_{eh}^N(\mathbf{r}, \mathbf{r}) = N^2 \frac{\|\psi_{N-1}\|^2}{\|\psi_N\|^2} P[\psi_N, \psi_{N-1}]. \quad (26)$$

The N^2 term accounts for the sum over all possible electron-hole pairs of the matrix elements O and P calculated for the recombination of one specific pair. $N[\psi_N, \psi_{N-1}] = \|\psi_{N-1}\|^2 / \|\psi_N\|^2$, is determined by importance sampling techniques.²³ A reasonable impor-

tance sampling probability density was obtained in terms of a model quasiexciton orbital $F_X(\mathbf{r}, \mathbf{s})$:

$$|\chi_N(R, S)|^2 = \frac{1}{N_P} \sum_P |F_X(P\mathbf{r}_1, P\mathbf{s}_1)|^2 \times |\psi_{N-1}(PR', PS')|^2, \quad (27)$$

$$\|\chi_N\|^2 = \|F_X\|^2 \|\psi_{N-1}\|^2,$$

where R and S denote the coordinates of all N electrons and holes, and P indicates a permutation of electron and hole coordinates in order to symmetrize χ_N . The estimator of $N[\psi_N, \psi_{N-1}]$ using $|\chi_N(R, S)|^2$ to sample $\{R, S\}$ is

$$N[\psi_N, \psi_{N-1}] = \|F_X\|^2 \left\langle \frac{|\psi_N(R, S)|^2}{|\chi_N(R, S)|^2} \right\rangle_X. \quad (28)$$

IV. ANALYSIS AND DISCUSSION

A. Recoil matrix element

We have calculated the quasiexciton orbital $Q_X(r)$ and coalesced electron-hole pair density $\tilde{\rho}_{eh}(r, r)$ using the exciton-gas-Jastrow polyexciton wave function [Eq. (4)]. Separate calculations of about 10 000 samples each were done for a coalesced electron-hole pair at a fixed distance from the center of mass of the other $N-1$ pairs. Errors for each point were quite small, in most cases less than 1%.

In Fig. 1 we plot quasiexciton orbitals $Q_X(r)$ for complexes with two, three, and four electron-hole pairs as a function of distance from the center of mass of the $N-1$ remaining pairs. The orbitals are almost identical for

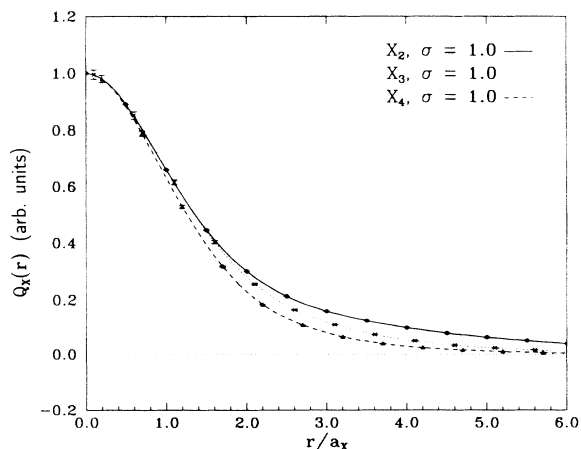


FIG. 1. Quasiexciton orbital for polyexcitons at zero electron-hole separation, measured as a function of distance from the center of mass of the rest of the complex. Normalization is arbitrarily set by fixing the orbital to 1.0 at the origin. Statistical errors are indicated by horizontal bars.

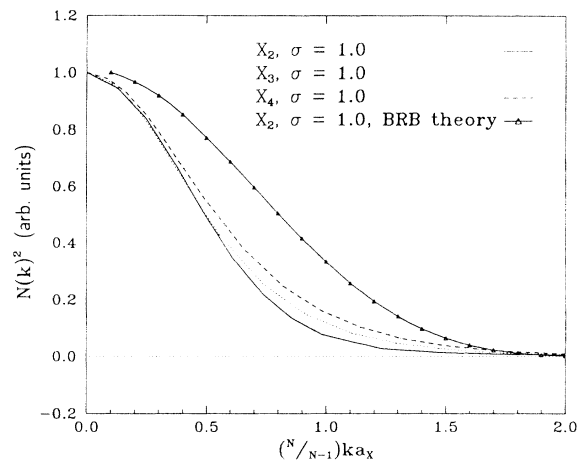


FIG. 2. Phonon recoil momentum probability distribution $|N(k)|^2$ for polyexcitons. Momentum is scaled by a factor of $\frac{N}{N-1}$ to show scaling behavior. Triangles denote the X_2 complex line shape using the variational theory of Brinkman, Rice, and Bell (BRB), taken from Ref. 2.

distances less than an exciton radius, with the X_2 showing a much longer asymptotic tail, consistent with its low exciton binding energy. Figure 2 shows the recoil probability $|N(k)|^2$ obtained from the square of the Fourier transform of $Q(r)$. Here it is convenient to plot $|N(k)|^2$ against the scaled momentum $\mathbf{k}' = \frac{N}{N-1}\mathbf{k}$. In this case we see that the recoil momentum distributions of each complex in terms of \mathbf{k}' are nearly identical. The function $N(\mathbf{k}')$ is the Fourier transform of the quasiexciton orbital [Eq. (13)] defined not in terms of the distance of the quasiexciton from the other $N-1$ pairs of the complex, but from the center of mass of the total N -pair complex. As mentioned earlier, the latter distance is equal to that of the former scaled by a factor of $\frac{N-1}{N}$. Thus each successively recombining electron-hole pair inhabits essentially the same quasiexciton orbital as the previous one, with the recoil energy of the final state changing each time only because it has less mass.

Kulakovski *et al.*² have used the variational wave function of Brinkman, Rice, and Bell¹⁹ to obtain the recoil momentum distribution for the X_2 , with the effective-mass overlap matrix element [Eq. (11)]. Their results are shown for comparison in Fig. 2. The recoil momentum cutoff is some 50–100% larger than that obtained with our wave function. It is probable that the large disagreement of the two matrix elements stems from the same kind of difficulty that underlay the calculation of the BX lifetime in Ref. 23.

B. Zero-temperature approximation

The role of the recoil matrix element in determining the PAL line shape is most marked in the limit of zero temperature. In the zero-temperature limit of Eq. (9) the Boltzmann factor is replaced by a δ -function at $\mathbf{K} = \mathbf{0}$ as the probability distribution for the initial X_N state. The resulting expression for the line shape is given by

$$I(\gamma) = \sum_k |N(k)|^2 \delta \left(\frac{\hbar^2 k^2}{2M(N-1)} - \gamma \right), \quad (29)$$

where γ is the photon energy shifted so that its zero lies at the transition energy for the bottom of the X_N band (taking the X_N total momentum $\mathbf{K} = \mathbf{0}$) to the bottom of the X_{N+1} band (total momentum $\mathbf{k} = \mathbf{0}$):

$$\gamma = \hbar\nu + \hbar\Omega(K_0) - E_{\text{gap}} - E_0[X_N] + E_0[X_{N-1}]. \quad (30)$$

At $T = 0$, only the kinetic energy of the final state plays a role in the line shape, and is proportional to the recoil energy between the phonon and $(N-1)$ complex. The PAL line shape thus becomes a direct measure of the momentum distribution of electron-hole pairs in the polyexciton.

Zero-temperature PAL line shapes for polyexcitons are shown in Fig. 3. The heavier masses of the larger X_N bring their line shape widths down to that of the biexciton, but have generally a longer low-energy tail. The predicted X_2 linewidth at half maximum for Si is roughly 0.7 meV assuming an exciton energy of 14.7 meV and exciton radius of 44.3 Å; this compares moderately well with the biexciton linewidth of 1.26 meV taken from the low-temperature experimental data of Thewalt and Rostworowski.¹

The $T=0$ line shape applies for temperatures corresponding to energies smaller than the typical recoil width of the PAL line, on the order of 10 K in Si. This is a temperature regime for which the EHL dominates the spectrum on the low-energy side of the free exciton line, and, in practice, only the biexciton line has been observed under these conditions. The effect of temperature on the X_2 line shape has been studied by Cho.⁶ At temperatures low compared to the recoil energy width, the line shape is convoluted with a Boltzmann distribution, adding an

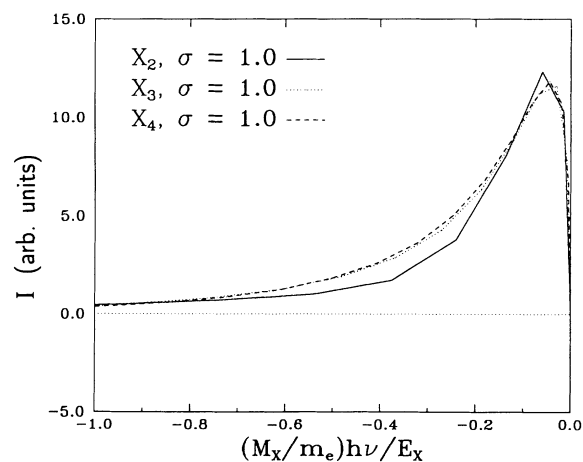


FIG. 3. Zero-temperature line shape for phonon-assisted luminescence from polyexciton complexes. Frequency measured relative to that of luminescence from the X_N band edge to the X_{N+1} band edge (zero kinetic energy for both states). Units are in terms of $m_e E_X / M_X$, the kinetic energy of an exciton with center-of-mass momentum a_X^{-1} .

exponential tail of width kT on the high-energy end of the line shape shown in Fig. 3. With increasing temperature, the growing Boltzmann tail slowly shifts the peak energy of the line to higher energies, until for temperatures comparable to the recoil energy the line shape is roughly symmetrical and centered at the high-energy edge of the zero-temperature line ($\gamma = 0$). Given similar linewidths for the X_3 and X_4 complexes, one may expect a transition to the high-temperature line shape to occur at roughly the same temperature as for the X_2 . With a recoil energy of about 1.25 meV for Si this translates into a temperature of 15 K, close to that of the EHL critical temperature. One expects polyexciton PAL luminescence near the EHL critical temperature to be characterized by broad, nearly symmetrical lines, with widths of 2–3 meV each. As the separation between each line is also on the order of a few meV, resolution of the luminescence of each individual line should be quite poor under practical conditions.

C. Oscillator strength of PAL

Figure 4 shows the (unnormalized) density of coalesced pairs in an N -pair complex as a function of pair distance from the center of mass of the rest of the complex. We calculate the total density of coalesced pairs from the integral of this function, divided by the normalization factors discussed in Sec. III. In Table I we show the integrated emission intensity I_{00} from the ground-state to ground-state process used to estimate the phonon-assisted line shape, and the intensity I_{tot} summed over all possible excited states of the final exciton complex. The deviation from 1 of the ratio of the ground-to-ground intensity to the total intensity measures the relative contribution of internally excited final states to the total observed emission. This is seen to be small. Alternately one may interpret this as determining the extent to which the transition is explainable in terms of the quasiexciton model for the recombining electron-hole pair. In partic-

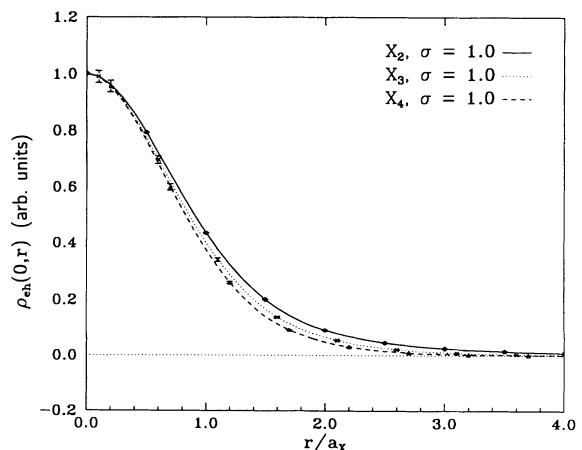


FIG. 4. Probability of coalescence of an electron-hole pair in the N -exciton complex, as a function of distance from the center of mass of the remaining $N-1$ pairs.

TABLE I. Integrated emission intensities for PAL from polyexcitons. Listed are number of excitons, integrated ground-state to ground-state intensity for electron-hole recombination (I_{00}), integrated intensity summed over all final states (I_{tot}), the fraction of the total intensity taken up by the ground-to-ground channel, and the total intensity per exciton. Also shown is the electron-hole contact density $\rho'_{eh}(0)$ extrapolated from the electron-hole two-particle density function. Errors in the last digits are shown in parentheses.

N	I_{00}	I_{tot}	I_{00}/I_{tot}	I_{tot}/N	$\rho_{eh}(0)$
1		0.3183		0.3183	0.3183
2	0.7180(20)	0.7216(20)	0.9948	0.3608(20)	0.733(15)
3	1.139(6)	1.328(5)	0.8579	0.4428(27)	1.317(22)
4	1.920(8)	2.080(8)	0.9229	0.5200(20)	2.096(32)

ular, we observe a very close fit for X_2 recombination by the transition to the ground state of the exciton. One possible explanation of this effect is that the exciton excitation spectrum is characterized by a large gap in energy, $0.75E_X$, between the ground and first excited $2p$ and $2s$ states. The X_2 , characterized by a very weak exciton binding energy of $0.05E_X$, should not mix in these excited states strongly. In addition, for configurations in which one pair is coalesced, our trial wave function biases the remaining electron-hole pair towards the exciton ground state. One expects that excited-state mixing will be less for the restricted region of configuration space important for pair recombination than on average. As final states, the X_2 and X_3 should have states at much lower excitation energies, starting at around the binding energy of the complex, consisting of low lying exciton scattering states or perhaps a weakly localized exciton bound by van der Waals interactions to the rest of the complex. Thus it is not surprising that final-state effects are more important in the larger complexes.

One can compare the oscillator strength of an N -pair complex to that of an equivalent system of N independent excitons by considering the oscillator strength per pair I_{tot}/N of each complex to the oscillator strength of a single exciton. Physically, this gives the density of holes in the vicinity of a given electron and is proportional to the oscillator strength for that electron to recombine with one of them. In the case of N noninteracting, isolated excitons, each electron may recombine with the hole bound to it in the exciton state with probability proportional to $|\phi_X(0)|^2$ and has essentially no probability of recombining with the other holes; the oscillator strength per pair of the noninteracting system is just the coalescence probability $1/\pi$ for the exciton ground state. The oscillator strength per exciton for polyexciton recombination is listed in Table I. We observe an oscillator strength that increases linearly with the number of pairs as

$$I_{\text{tot}}/N = 0.8\pi + (N - 1)0.11. \quad (31)$$

Each electron in the polyexciton is strongly correlated with one hole, as in the isolated exciton, and experiences a weaker, screened, correlation with each of the remaining holes in the system.

Finally we note that the total oscillator strength I_{tot} is identical to $\rho_{eh}(0)$, the electron-hole two-particle density for $r = 0$, defined as

$$\rho_{eh}(0) = \sum_i^N \sum_j^N \langle \delta(\mathbf{r}_i - \mathbf{s}_j) \rangle. \quad (32)$$

This factor can be independently calculated using a simple binning procedure. One can sample the variational wave function ψ_N to obtain M configurations of the N -pair polyexciton and calculate the fraction of electron-hole pairs that fall within a range $\{r, r + \delta\}$ of each other. The result is a histogram plot of the two-body density $\rho_{eh}(r)$. Using this method to estimate $\rho_{eh}(0)$ is quite inefficient since the large majority of particle pairs sampled will lie at distances outside any reasonable bin radius δ at the origin. However, cusp conditions on the two-body density at small distances can be utilized to extrapolate the distribution function to a reasonable value at zero. Estimates for the coalescence density $\rho_{eh}(0)$ using this extrapolation method are shown in the last column of Table I. These are in good agreement with the coalescence densities measured by the importance sampling method outlined in this paper, providing a strong check of the method.

D. Discussion

Two main possibilities for error in the line shape and integrated intensities occur. One is the result of inaccuracies in the variational wave function used to describe the effective-mass ground state. In particular, the asymptotic behavior of the polyexciton wave function as one removes an electron-hole pair far from the rest of the complex has been only roughly modeled. The discrepancy between our calculated linewidth and that observed experimentally is at least to some degree caused by the choice of our trial wave function. Our model is exact for loosely bound complexes and deals only approximately with the three- and four-body correlations that should be important for short-range configurations, and account for a significant fraction of the binding energy. As a result the variationally optimized wave function obtained with the current model should overestimate the volume of the PE and underestimate its recoil linewidth. A previous study of the effect of correlations on the bound exciton lifetime shows that their inclusion greatly effects the recombination matrix element, with a variation of almost two orders of magnitude from a Heitler-London model to

a nearly exact wave function.²³

The other consideration is the accuracy of the effective-mass model itself. To what extent is the effective-mass calculation of $\rho_{eh}(0)$ reasonable considering that it is accurate only in the long-wavelength limit? One expects some distortion of the electron-hole wave function when the electron and hole are within a unit cell or two of each other, precisely the region which determines recombination matrix elements. As a result, the total lifetime measurement cannot be considered to be quantitatively accurate, and may be off by an order of magnitude without significant changes in the binding energy of the complex, which would depend much more on the behavior of the wave function at average electron-hole separations. On the other hand, the line shape should not suffer as much from this limitation. It depends on the relative change in the overlap matrix element as one pulls the recombining electron-hole pair away from the rest of the complex, and is peaked about wavelengths of several exciton radii. The presence of such long-wavelength correlations with other particles should not influence too strongly the nature of the correction of the effective-mass matrix element due to the electron-hole interaction at very short distances. This kind of correction can then be absorbed into the definition of the phonon matrix element D_{cv} without too much consequence to the calculation of line shapes or intensity ratios such as I_{00}/I_{tot} .

V. CONCLUSION

This paper reports the calculation by variational Monte Carlo methods of the line shape and oscillator strength of the phonon-assisted photoluminescence from polyexciton complexes. The polyexciton PAL line shape of polyexcitons is found to be modeled well by the treatment of the recombining pair as an uncharged Bose quasiparticle. In a sense, this is caused by the projection of the properties of the phonon onto the recombining electron-hole pair in the phonon-assisted transition. We find, as expected for a quasiexciton picture, that the ground-state to ground-state transition is the dominant channel for phonon-assisted decay. In addition, the probability density of the quasiexciton orbital varies only slightly with the number of excitons in the complex, allowing for a very simple model of the line shape. Calculated line shapes show a rough independence of the number of electron-hole pairs in the complex, with oscillator strengths per pair increasing gradually with number of pairs.

The line shapes calculated here are a starting point towards a quantitative characterization of the luminescence from these complexes. There are two lines along which improvements can be made: employing a trial wave function that has a more accurate treatment of interparticle correlations, and the inclusion of realistic band-structure effects such as anisotropies and spin-orbit and valley-orbit interactions. Like the bound exciton wave function we have previously studied in Ref. 23, the wave function probably overestimates the volume of the center-of-mass motion of the recombining exciton about the rest of the complex. As a result, the peak intensity of the PAL line shape is probably overestimated with particular overem-

phasis of the small-wave-number components. The deviation of the band structure of Si from the spherical bands considered here should also affect the observed linewidth. In general, the experimentally observed binding energies for the complexes are deeper than their theoretical counterparts, leading to the expectation that the typical recoil energy should be larger and the PAL linewidth broadened with realistic band-structure effects. At present, the experimental data for the larger complexes cannot be easily compared with since they include the unresolved contributions of several species of polyexcitons, most likely with a background of electron-hole plasma as well. Further experimental probes of the metal-insulator transition in electron-hole plasmas may be necessary to understand the nature of the intermediate density regime.

ACKNOWLEDGMENTS

We would like to thank J. P. Wolfe and Gerardo Ortiz for fruitful discussions. This work was supported by the Office of Naval Research (ONR) under Contract No. N00014-89-5-1157 and the National Science Foundation. We acknowledge the use of the Cray Research, Inc., Y-MP/48 computer at the National Center for Supercomputing Applications at the University of Illinois, and the computing facilities of the University of Illinois Materials Research Laboratory.

APPENDIX: DERIVATION OF THE EFFECTIVE MASS PAL MATRIX ELEMENT

A derivation of the matrix element for phonon-assisted luminescence is easily obtained starting with a minimalist model of the phonon-assisted radiative recombination in which an electron-hole pair with total momentum $\mathbf{k}_e + \mathbf{k}_h = \mathbf{q}$ is annihilated to create a photon-phonon pair with the same total momentum. We consider a general "black box" form for this interaction, $V_{\text{eff}}(\mathbf{k}_e, \mathbf{k}_h, \mathbf{q}, 0)$, assuming nothing about the detailed nature of the separate phonon and photon emission processes but conservation of momenta, e.g., ignoring umklapp processes. This kind of interaction can be derived by summing over the intermediate states of the second-order perturbation theory process described in Sec. II or from alternate models of phonon emission such as the exciton-phonon coupling model used by Cho.⁶ This interaction can be treated as a perturbation to the polyexciton Hamiltonian of the form

$$V = \sum_{\mathbf{k}_e, \mathbf{k}_h, \mathbf{q}} V_{\text{eff}}(\mathbf{k}_e, \mathbf{k}_h, \mathbf{q}, 0) a_{\mathbf{k}_e} b_{\mathbf{k}_h} d_{\mathbf{q}}^\dagger c_0^\dagger, \quad (\text{A1})$$

where a , b , c , and d are electron, hole, photon, and phonon destruction operators respectively.

Assuming this form of interaction, the phonon-assisted recombination matrix element may be determined using first-order perturbation theory techniques similarly to the single-photon emission process in direct-gap recombination. In particular, consider an indirect-gap exciton of total momentum \mathbf{K} and internal excitation state denoted by τ ,

$$|\tau, \mathbf{K}\rangle = \sum_{\mathbf{k}, \mathbf{k}'} F^\tau[(\mathbf{k} - \mathbf{k}')/2] \times \delta(\mathbf{K}, \mathbf{k} + \mathbf{k}') a_{\mathbf{k}_{c0} + \mathbf{k}}^\dagger b_{\mathbf{k}_{v0} + \mathbf{k}'}^\dagger |0\rangle, \quad (\text{A2})$$

where electron and hole momenta have been defined relative to those of the conduction and valence band extrema, \mathbf{k}_{c0} and \mathbf{k}_{v0} . One obtains for the matrix element for recombination to the crystal ground state

$$\langle 0 | V_{\text{eff}} | n, \mathbf{K} \rangle = \sum_{\mathbf{k}, \mathbf{k}'} V_{\text{eff}}(\mathbf{k}_{c0} + \mathbf{k}, \mathbf{k}_{v0} + \mathbf{k}', \mathbf{q}, 0) \times F^\tau[(\mathbf{k} - \mathbf{k}')/2] \delta(\mathbf{K}, \mathbf{k} + \mathbf{k}'). \quad (\text{A3})$$

At temperatures low enough for the exciton to be bound, both the thermal distribution of the total momentum \mathbf{K} and the spread of relative momenta described by the electron-hole correlation envelope F^τ are of order of an inverse exciton radius, a_X^{-1} . As with the direct emission process, one can thus assume that the coupling $V_{\text{eff}}(\mathbf{k}_{c0} + \mathbf{k}, \mathbf{k}_{v0} + \mathbf{k}', \mathbf{q}, 0)$ varies slowly over the range of \mathbf{k} and \mathbf{k}' important for the determination of the matrix element and can be represented by a constant $D_{cv} = V(\mathbf{k}_{v0}, \mathbf{k}_{c0})$. With this approximation and taking a Fourier transform of the matrix element coordinates, one obtains the following expression for the recombination matrix element:

$$\langle 0 | V_{\text{eff}} | n, \mathbf{K} \rangle = D_{cv} \int F^\tau(\tau) \exp(i\mathbf{k} \cdot \mathbf{R}) \delta(\mathbf{r}) d\mathbf{R} d\tau. \quad (\text{A4})$$

The effective-mass phonon-assisted recombination matrix element is thus an extension of Elliott's theory for exciton absorption,¹⁸ with the phonon playing the passive role of relaxing the $\mathbf{K} = \mathbf{0}$ constraint of the direct-gap process.

The extension of (A4) for the transition matrix element

$$\langle RS | a_{\frac{\mathbf{q} + \mathbf{k}}{2}}^\dagger b_{\frac{\mathbf{q} - \mathbf{k}}{2}}^\dagger | N - 1, \tau', \mathbf{K}' \rangle = S \{ \exp[i(\mathbf{K}' + \mathbf{q}) \cdot \mathbf{R}_N] \exp[i(\frac{N-1}{N}\mathbf{q} - \frac{1}{N}\mathbf{K}') \cdot \mathbf{R}] \times \exp[i\mathbf{k} \cdot (\mathbf{r}_1 - \mathbf{s}_1)] \phi^{\tau'}(\mathbf{r}_2, \dots, \mathbf{r}_N, \mathbf{s}_2, \dots, \mathbf{s}_N) \}. \quad (\text{A8})$$

The matrix element for PAL is now given by the integral over spatial coordinates R and S for the holes and electrons of the product of the two terms (A8) and (A6). One obtains, after integrating over the center-of-mass co-

ordinate between the N -exciton and the $N-1$ -exciton + phonon + photon complex proceeds as follows. For an initial electronic state $|N, \tau, \mathbf{K}\rangle$, of N electron-hole pairs with total momentum \mathbf{K} and internal quantum number τ plus N_q phonons with momentum \mathbf{q} and N_0 zero-momentum photons, and a final electronic state $|N-1, \tau', \mathbf{K}'\rangle$, the matrix element is given by

$$M(\mathbf{K}', \mathbf{q}, \mathbf{K}) = \sqrt{N_q + 1} \sqrt{N_0 + 1} \langle N - 1, \tau', \mathbf{K}' | \times \sum_{\mathbf{k}} V(\mathbf{k}, \mathbf{q}) a_{\frac{\mathbf{q} + \mathbf{k}}{2}} b_{\frac{\mathbf{q} - \mathbf{k}}{2}} | N, \tau, \mathbf{K} \rangle. \quad (\text{A5})$$

To obtain an expression in (first quantized) coordinate space for the Monte Carlo calculation, one may use the expressions

$$\langle RS | N, \tau, \mathbf{K} \rangle = \langle \mathbf{r}_1, \dots, \mathbf{r}_N, \mathbf{s}_1, \dots, \mathbf{s}_N | N, \tau, \mathbf{K} \rangle = \exp(i\mathbf{K} \cdot \mathbf{R}_N) \phi^\tau(\mathbf{r}_1, \dots, \mathbf{r}_N, \mathbf{s}_1, \dots, \mathbf{s}_N), \quad (\text{A6})$$

where \mathbf{R}_N is the center of mass of the N -pair system and ϕ^τ involves relative coordinates, and

$$\langle RS | a_{\frac{\mathbf{q} + \mathbf{k}}{2}}^\dagger b_{\frac{\mathbf{q} - \mathbf{k}}{2}}^\dagger | N - 1, \tau', \mathbf{K}' \rangle = S [\exp(i\frac{\mathbf{q} + \mathbf{k}}{2} \cdot \mathbf{r}_1) \exp(i\frac{\mathbf{q} - \mathbf{k}}{2} \cdot \mathbf{s}_1) \exp(i\mathbf{K}' \cdot \mathbf{R}_{N-1}) \times \phi^{\tau'}(\mathbf{r}_2, \dots, \mathbf{r}_N, \mathbf{s}_2, \dots, \mathbf{s}_N)], \quad (\text{A7})$$

where \mathbf{R}_{N-1} is the center-of-mass coordinate of the $N-1$ -pair complex and S is the symmetrization operator. Given that $\phi^{\tau'}$ is independent of \mathbf{R}_{N-1} and \mathbf{R}_N , one can rewrite the second state in terms of three components, one involving \mathbf{R}_N , another the distance between the center of mass of the recombining pair and that of the $N-1$ -pair subsystem, $\mathbf{R} = \frac{(\mathbf{r}_1 + \mathbf{s}_1)}{2} - \mathbf{R}_{N-1}$, and one involving the relative coordinates of the single and $N-1$ -pair states. The expression is then given by

ordinate \mathbf{R}_N , the expression for the internal recoil of the electron-hole pair and X_{N+1} complex as given by Eq. (11) and a conservation of total momentum term $\delta(\mathbf{K}' + \mathbf{q} - \mathbf{K})$.

¹M. L. W. Thewalt and J. A. Rostworowski, *Solid State Commun.* **25**, 991 (1978).

²V. D. Kulakovskii, V. B. Timofeev, and V. M. Edelstein, *Zh. Eksp. Teor. Fiz.* **74**, 372 (1978) [*Sov. Phys. JETP* **47**, 193 (1978)].

³I. V. Kukushin, V. D. Kulakovskii, and V. B. Timofeev, *Pis'ma Zh. Eksp. Teor. Fiz.* **32**, 304 (1980) [*JETP Lett.* **32**, 280 (1980)].

⁴J. R. Haynes, *Phys. Rev. Lett.* **17**, 860 (1966).

⁵V. M. Asmin and A. A. Rogachev, *Pis'ma Zh. Eksp. Teor. Fiz.* **7**, 464 (1968) [*JETP Lett.* **7**, 360 (1968)].

⁶K. Cho, *Opt. Commun.* **8**, 412 (1973).

⁷J. C. Culbertson and J. E. Furneaux, *Phys. Rev. Lett.* **49**, 1528 (1982).

⁸C. Benoit à la Guillaume, M. Voos, and F. Salvan, *Phys. Rev. B* **5**, 3079 (1972).

⁹*Electron Hole Droplets in Semiconductors*, edited by C. D. Jeffries and R. V. Keldysh (North-Holland, Amsterdam, 1983).

¹⁰P. Vashishta and R. K. Kalia, in *Electron Hole Droplets in Semiconductors* (Ref. 9), p. 21.

¹¹T. M. Rice, in *Solid State Physics: Advances in Research*

- and Applications*, edited by H. Ehrenreich, F. Seitz, and D. Turnbull (Academic Press, New York, 1977), Vol. 32.
- ¹²N. F. Mott, *Metal Insulator Transitions* (Taylor and Francis, London, 1974).
- ¹³M. Combescot, Phys. Rev. Lett. **32**, 15 (1974).
- ¹⁴L. M. Smith and J. P. Wolfe, Phys. Rev. Lett. **57**, 2314 (1986).
- ¹⁵A. H. Simon, S. J. Kirch, and J. P. Wolfe, Phys. Rev. B **46**, 10 098 (1992-II).
- ¹⁶A. G. Steele, W. G. McMullan, and M. L. W. Thewalt, Phys. Rev. Lett. **59**, 2899 (1987).
- ¹⁷V. B. Timofeev, in *Excitons*, edited by M. D. Sturge and E. I. Rashba (North-Holland, Amsterdam, 1982), p. 349.
- ¹⁸R. J. Elliott, Phys. Rev. **108**, 1384 (1957).
- ¹⁹W. F. Brinkman, T. M. Rice, and B. Bell, Phys. Rev. B **8**, 1570 (1973).
- ²⁰M. A. Lee, P. Vashishta, and R. K. Kalia, Phys. Rev. Lett. **51**, 2422 (1983).
- ²¹A. C. Cancio and Y. C. Chang, Phys. Rev. B **42**, 11 317 (1990).
- ²²T. Chakroborty and P. Pietilainen, Phys. Rev. Lett. **49**, 1034 (1982); P. Pietilainen, L. Lantto, and A. Kallio in *Recent Progress in Many Body Theories*, edited by H. Kümmel and M. L. Ristig, Lecture Notes in Physics Vol. 198 (Springer Verlag, Berlin, 1984), p. 181.
- ²³A. C. Cancio and Y. C. Chang, Phys. Rev. B **47**, 13 246 (1993).
- ²⁴D. S. Lewart, V. R. Pandaripandhe, and S. C. Pieper, Phys. Rev. B **37**, 4950 (1988).
- ²⁵O. Benhar, V. R. Pandaripandhe, and Steven C. Pieper, Rev. Mod. Phys. **65**, 817 (1993).
- ²⁶See, for example, D. M. Ceperley and M. H. Kalos, in *Monte Carlo Methods in Statistical Physics*, edited by K. Binder (Springer-Verlag, Berlin, 1979).
- ²⁷The time required by this method is quite reasonable given the ease of calculating the wave functions of these relatively small complexes. For larger systems, weighting methods for selecting r can be used to provide greater resolution of the orbital function where it is largest, and rougher estimates for larger r .